SCWO OF SALT-CONTAINING ARTIFICIAL WASTEWATER USING A TRANSPIRING-WALL REACTOR

Ph. Rudolf von Rohr*, K. Prikopsky and B. Wellig[1]
Institute of Process Engineering, Swiss Federal Institute of Technology (ETH), CH-8092 Zurich, Switzerland
*E-mail: vonrohr@ipe.mavt.ethz.ch, Fax: +41 (0) 44-632 13 25, www.ipe.ethz.ch.
[1]Present address: Ernst Basler+Partner AG, Mühlebachstrasse 11, CH-8032 Zurich, Switzerland.

INTRODUCTION

Supercritical Water Oxidation (SCWO) is a high-pressure high-temperature process for the destruction of toxic, hazardous and/or non-biodegradable aqueous organic waste. SCWO is carried out at conditions above the critical point of pure water (T_c=374°C and p_c=221 bar). As a result of the complete miscibility of organic substrates and gases in supercritical water (SCW), high reaction rates and conversions close to unity can be achieved. The thermophysical properties of water near and above its critical point change significantly compared to ambient conditions. Water, which is polar in the liquid state, is much less polar in its critical state and becomes a good solvent to non-polar compounds and gases such as oxygen, nitrogen or carbon dioxide [1-3]. The lack of interfacial mass transfer resistances in such a single-phase mixture (under salt-free conditions) combined with high reaction temperatures, leads to short residence times and small reactor volumes (*i.e.*, high space-time yields). Corrosion of reaction vessels and process equipment when employing SCW combined with reactive ions such as Cl^-, F^-, H_3O^+ and oxygen is one of the major challenges that the use of this technology needs to address [4-9]. Besides corrosion, the problem of equipment plugging due to precipitation of salt particles in SCW is the most severe problem that SCWO processes face nowadays [6]. The solubility of inorganic salts in SCW decreases sharply when exceeding the critical point of water [10-12]. Agglomerates of precipitated salts formed during operation adhere to reactor walls and change flow and heat transfer conditions across the reactor walls.

A transpiring-wall reactor [13-16] containing a hydrothermal flame was investigated in this work using various analyzing methods. The so-called "hydrothermal flames" have been observed in semi-batch reactors [17-23] and have been also successfully investigated in continuously operated reactors [13-16, 24, 25]. The hydrothermal flame provides desired reaction temperatures operating at subcritical inlet temperatures, which reduces corrosion and avoids plugging (when introducing salt-containing waste water) of the reactor inlet lines. Precipitated salt is either redissolved or flushed away by the water film formed on the inner surface of the transpiring-wall.

The aim of the experiments in the present work was to find optimal operating conditions of the facility in order to overcome plugging of the reactor or its components.

I - MATERIALS AND METHODS

Figure 1 shows the sectional drawing of the transpiring-wall reactor. The vertical reactor vessel made of nickel-based Alloy 625 has an inner diameter of 34mm and a transpiration zone length of 375mm. The vessel was designed to sustain burst pressures up to 600bar and temperatures up to 600°C. The coaxial burner setup in the upper zone of the reactor consists of a burner tube, combustion chamber and an outer insert made of Alloy 625 and separates the

fuel, oxygen and wastewater inlet stream of the reactor (see also Fig. 3). The burner tube is an air-gap-insulated double-tube system, where the inner tube and the burner nozzle were fabricated using Alloy 230.

High-porous cylindrical elements (sintered Alloy 625 GKN Sinter Metals Filters, Radervormwald, Germany) with an inner diameter of 22mm and a thickness of 3.75mm form the transpiring-wall. The transpiration zone is divided into four separate sections. In the first three sections (TW1, TW2, TW3) the transpiring water was introduced, while in the last section (CW) cooling water was supplied. The advantage of this setup is the possibility to control the mass flow rates of the transpiring water flows and temperatures for each section separately. The elements are easy to replace and different tube porosities can be employed. We used sinter tube elements with a porosity of 17% (equivalent laminar diameter of 3µm) and 21% (equivalent laminar diameter of 5µm) in our experiments.

Furthermore, three intermediate rings made of Alloy 625 allowed a lead-through of thermocouples into the transpiration zone. Radial temperature profiles at three different heights (planes P2, P3, P4) were measured. The disadvantage of this setup was the disturbance of the flow through the integrated thermocouples in the inlet and transpiration zone of the reactor and salt adherence on the thermocouples. Further measuring points are shown in Fig.1. Four conveyor units were used for pressurizing the downstream reactor. The system pressure was measured with a pressure transducer and controlled using a PI controller. Mass flow rates of the fuel (F_f), oxygen (F_{ox1}, F_{ox2}), wastewater (F_{ww}), transpiring water (F_{tw1}, F_{tw2}, F_{tw3}) and cooling water (F_{cw}) flows were measured by means of Coriolis-type mass flow meters and adjusted manually. Exactly adjustable fluid temperatures up to 600°C were achieved using electric resistance high-pressure pre-heaters [15] and controlled using PID controllers. Further detailed information about the setup can be found elsewhere [15, 16].

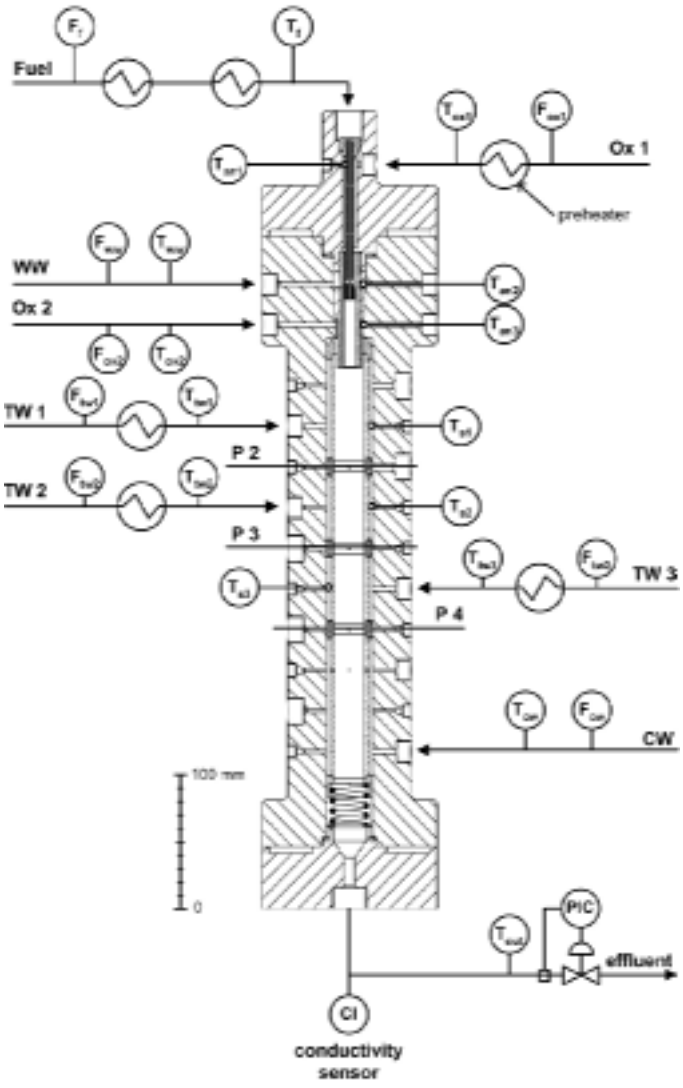

Figure 1: Sectional drawing of the transpiring-wall reactor and pilot plant configuration used in this work. Descriptions of mass flow rate and reactor inlet temperature measurements are provided in Tab. 1. Further measuring points: T_{bn} = fuel temperature in the burner nozzle (some millimeters above the tip of the burner tube), T_{an1} = Ox1 temperature in the inner annular gap, T_{an2} = WW temperature in the middle annular gap, T_{an3} = Ox2 temperature in the outer annular gap, T_{si} = TW temperature in the annular gap of section i (i = 1 - 3), CI = on-line conductivity and temperature measurement of reactor effluent, T_{out} = temperature of reactor effluent. Modifications in the CW section were provided in comparison to the setup presented in Ref. [15, 16].

Desalinated water-methanol mixtures were used as fuel flow for the hydrothermal flame. Methanol (Synopharm, Schweizerhalle, Basel, Switzerland, purity > 99.8%) was chosen as model organic compound. The electric conductivity of the used desalinated water at ambient conditions was 0.6-0.9μS. Technical grade oxygen (PanGas, Dagmersellen, Switzerland, purity > 99.5%) was used as oxidizer. The artificial wastewater consisted of 6wt.% methanol and up to 3wt.% sodium sulfate (Sigma-Aldrich Laborchemikalien GmbH, Seelze, Germany, anhydrous, purity ≥ 99%).

II - EXPERIMENTAL PROCEDURE

All experiments were carried out at a constant pressure of 250bar. The methanol mass fraction in the fuel flow w_f was 16wt.% and 22wt.%. The artificial wastewater stream contained w_{ww}=6wt.% methanol. The mass fraction of sodium sulfate $w_{salt,in}$ was set to 1wt.% and 3wt.% within the artificial wastewater mixture. For the transpiring and cooling water flow, desalinated water was used. The first step of an experiment was the ignition of the hydrothermal flame under salt-free conditions. The ignition occurred about 20 to 30 minutes after the start-up, when inlet temperatures of the fuel and of the oxygen flow (T_f and T_{ox1}) reached values up to 460°C. After ignition, these temperatures were set to desired subcritical values. Mass flow rates (F_f , F_{ox1}, F_{ww}, F_{ox2}, F_{tw1}, F_{tw2}, F_{tw3}, F_{cw}) and temperatures of the transpiring water flow (T_{tw1}, T_{tw2}, T_{tw3}) were adjusted and kept constant and a switch-over to a wastewater mixture of defined salt and methanol content was performed. In Table 1 all flows entering the transpiring-wall reactor are summarized. The conductivity signal was monitored and provided qualitative information about the salt deposition in the reactor. The *transpiration intensity* κ was a suitable criterion for adjusting the mass flow rates of the transpiring water flows and was defined as the ratio between the mass flux of each transpiring flow and the bulk mass flux at the entrance of the transpiring-wall tube (combustion products + wastewater + oxygen 2):

$$\kappa_i = \frac{F_{twi}/A_{twi}}{(F_f + F_{ox1} + F_{ww} + F_{ox2})/A_b} = \frac{F_{twi}/A_{twi}}{F_b/A_b} \tag{1}$$

A_b and A_{twi} are the inner circular area and the inner shell surface of the sinter tube, respectively. The geometric data can be found elsewhere [15, 16].

The transpiration intensity was varied from 1% to 6% in the experiments. The duration of stationary conditions in the experiments lasted from 20 minutes up to 3 hours. During this phase, the liquid reactor effluent was collected in samples. After completion of an experiment, the wastewater flow was switched to desalinated water. Fuel and oxygen temperatures were lowered to extinction and the fuel stream was switched to desalinated water. The plant had to be cooled down for 15 to 30 minutes before the pressure was reduced stepwise. To avoid influence of the salt residue on the next experiment, the reactor was rinsed with water after an experiment until the conductivity value of the on-line sensor reached steady values, equal to those obtained prior conducting the experiment. The whole system was left filled with desalinated water until the next run. After the experiment, liquid samples were analyzed. To determine the salt deposition in the reactor, the conductivity in the reactor effluent was measured on-line (described below) and offline (HI 8733 conductivity meter, Hanna Instruments, Germany). Additionally, an ionic chromatography device (Dionex DX-120 equipped with Ionpac CS12A cation exchange column and cation suppressor, Dionex Corporation, USA) was used to determine the concentration of sodium in the samples.

Analysis of the conversion of the organic compound was provided by a gas chromatograph equipped with a flame ionization detector (GC-FID, Hewlett Packard, 5890 Series II).
The on-line conductivity sensor was placed in the reactor effluent and allowed a simultaneous in-situ electric conductivity and temperature measurements at high pressure and temperature [14]. The conductivity is a function of the amount of ions within a solution and shows a linear behavior for low ion concentrations. Besides, temperature and pressure can further affect the conductivity of a solution. The influence of pressure was not investigated, since all experiments were performed at a constant pressure of 250bar. A calibration of the conductivity sensor was provided with respect to salt concentrations and temperatures in the reactor effluent expected in experiments using salt-containing artificial wastewater. Furthermore, it was necessary to provide a correction of the measured conductivity value. Thus, the conductivity increase caused by the production of CO_2 (production of ions) was subtracted from the measured conductivity value.

Flow	Index	Mass flow rate	Inlet temperature
fuel (water-MeOH)	f	$F_f \approx 1.5$g/s	$T_f \approx 345 – 370$°C
Ox 1: oxygen 1	ox1	$F_{ox1} \approx 1.5\gamma F_f w_f$	$T_{ox1} \approx 395 – 430$°C
WW: wastewater (water-MeOH-Na_2SO_4)	ww	$F_{ww} \approx 1.0$g/s	$T_{ww} \approx 20$°C
Ox 2: oxygen 2	ox2	$F_{ox2} \approx 0.17$ - 0.25g/s	$T_{ox2} \approx 30 – 35$°C
TW 1: transpiring water 1	tw1	$F_{tw1} = \kappa_1 F_b A_{tw1}/A_b$	$T_{tw1} \approx 75 – 200$°C
TW 2: transpiring water 2	tw2	$F_{tw2} = \kappa_2 F_b A_{tw1}/A_b$	$T_{tw2} \approx 75 – 200$°C
TW 3: transpiring water 3	tw3	$F_{tw3} = \kappa_3 F_b A_{tw1}/A_b$	$T_{tw3} \approx 75 – 200$°C
CW: cooling water	cw	$F_{cw} \approx 55 – 70$g/s	$T_{cw} \approx 28 – 35$°C

Table 1: Summary of all flows entering the transpiring-wall reactor (see Fig. 1) and their mass flow rates F_i and inlet temperatures T_i. Nomenclature: γ = stoichiometric oxygen excess for hydrothermal flame = $F_{ox1}/(\varphi_{O2} F_f w_f) \approx F_{ox1}/(1.5 F_f w_f)$, $\varphi_{O2} = (v_{O2} M_{O2})/(v_{CH3OH} M_{CH3OH}) \approx 1.5$, v_i and M_i are the stoichiometric coefficient and the molar mass of compound i, w_f = 16-22wt.% = methanol mass fraction in the fuel flow, w_{ww} = 6wt.% = methanol mass fraction in the wastewater flow, κ_i = transpiration intensity in section i, A_{twi}= inner shell surface of the sinter tube of section i, A_b = inner circular area, F_b =mass flow rate of bulk stream ($F_b = F_f + F_{ox1} + F_{ww} + F_{ox2}$).

The results of conductivity and ionic chromatography measurements $w_{salt,out}$ were used to calculate the salt deposit fraction χ_{salt}. The salt deposit fraction indicated how many percent of the metered salt ($w_{salt,in} F_{ww}$) was deposited in the reactor and is defined by the following equation:

$$\chi_{salt} = 1 - \frac{w_{salt,out}(F_f(1 - w_f + w_f \varphi_{H2O}) + F_{ww}(1 - w_{ww} - w_{salt,in} + w_{ww} \varphi_{H2O}) + F_{tw1} + F_{tw2} + F_{tw3} + F_{cw})}{w_{salt,in} F_{ww}} \tag{2}$$

$\varphi_{H2O} = (v_{H2O} M_{H2O})/(v_{CH3OH} M_{CH3OH}) \approx 1.125$ and v_i and M_i are the stoichiometric coefficient and the molar mass of compound i respectively. When a complete conversion of methanol to CO_2 and H_2O is assumed, $F_f w_f \varphi_{H2O} + F_{ww} w_{ww} \varphi_{H2O}$ is the amount of water generated by the oxidation reaction:

$$CH_3OH + \frac{3}{2} O_2 \rightarrow CO_2 + 2H_2O \tag{3}$$

The error made by this simplification is negligible compared to the uncertainties of mass flow, conductivity measurements and of the chemical analysis of the effluent.

III – RESULTS

Two main sets of experiment series have been carried out using different transpiring-wall elements with porosities of 17% and 21%. The influence of the transpiration intensity κ_i and the inlet temperatures T_{twi} of the transpiring water flows (TW1, TW2, TW3) on the salt deposit fraction in the reactor was experimentally investigated. The results of the experiments are shown in Fig. 2. The stationary conditions with salt-containing artificial wastewater lasted up to 3 hours. No plugging of the reactor or a pressure drop increase across the transpiring-wall could be detected. In experiments using elements with the lower porosity only the conductivity sensors were used to determine the salt concentrations in the reactor effluent. In further experiments (elements with porosity of 21%) ionic chromatography was employed additionally to analyze liquid samples. Salt deposit fraction up to 30 % was detected. The parameters κ_i and T_{twi} did not show significant influence on the salt deposition even at high transpiration intensities (κ_i = 6) and the results using conductivity sensors and ionic chromatography were in a good agreement considering the error bars of the results.

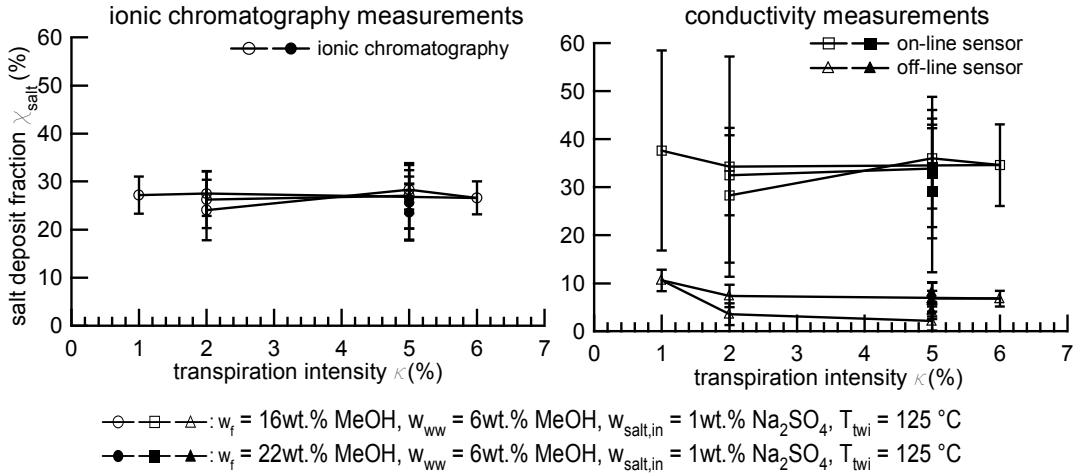

Figure 2: Results from experiments using transpiring-wall elements with the porosity of 21%.

The on-line conductivity signal fluctuated strongly during stationary conditions and mainly contributed to the uncertainty of the results. Further sources of error were the mass flow rate and temperature fluctuations and a salt residue left in the reactor after an experiment. Since the influence of the transpiration intensity was negligible, the upper flame/hot zone of the reactor was a region of supposed salt deposition. In the gap between the burner chamber and the outer insert salt residues were found after the dismantling of the reactor. We assume supercritical temperatures in this region with respect to the results obtained using salt-free artificial wastewater [15, 16]. The region of found and supposed salt deposition at the burner setup is shown in the Fig. 3.

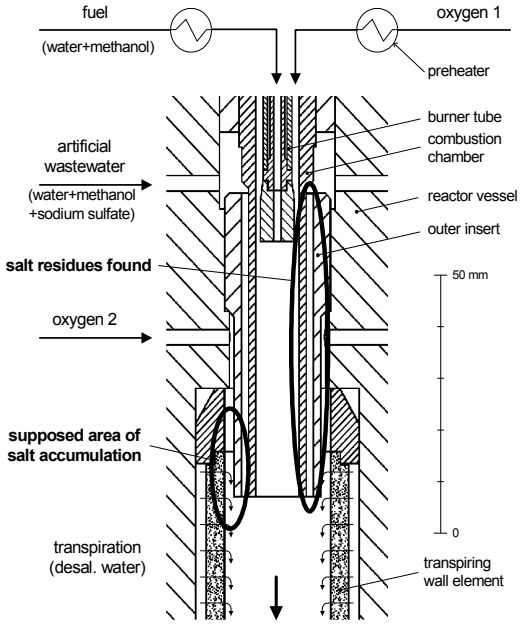

Figure 3: Region of found and supposed salt deposition at the burner setup.

CONCLUSION

In this work we investigated the performance of the transpiring-wall reactor with a hydrothermal flame as internal heat source in order to overcome plugging of the reactor or its components. Artificial wastewater streams used in the experiments contained up to 3wt.% of sodium sulfate. The concept using the hydrothermal flame and the transpiring-wall worked satisfactory. No plugging of the reactor was observed during the experiments. However, salt deposition was detected in the upper hot zone of the reactor. A sophisticated burner design could overcome these problems. The results of the conductivity sensors and of ionic chromatography were in a good agreement. When using conductivity sensors, the influence of various parameters (e.g. production of ions due chemical reactions) on conductivity has to be considered.

ACKNOLEDGMENTS

This work was funded by ETH Zurich and Swiss National Science Foundation (SNF).

REFERENCES:

[1] Brunner, E., J. Chem. Thermodyn., Vol. 22, **1990**, p. 335
[2] Japas, M.L., Franck, E.U., Ber. Bunsen-Ges. Phys. Chem. Chem. Phys., Vol. 89, **1985**, p. 1268
[3] Franck, E.U., In: Supercritical fluids - fundamentals and applications, Kiran, E., Debenedetti, P.G., and Peters, C.J. (Eds.), Kluwer Academic Publishers, Dodrecht, The Netherlands, **2000**, p. 307
[4] Konys, J.*, et al.*, Corrosion, Vol. 55, **1999**, p. 45
[5] Kritzer, P., Boukis, N., Dinjus, E., Corrosion, Vol. 56, **2000**, p. 1093
[6] Kritzer, P., Dinjus, E., Chem. Eng. J., Vol. 83, **2001**, p. 207
[7] Mitton, D.B.*, et al.*, Ind. Eng. Chem. Res., Vol. 39, **2000**, p. 4689
[8] Mitton, D.B.*, et al.*, Mater. Technol., Vol. 16, **2001**, p. 44
[9] Kritzer, P., J. Supercrit. Fluids, Vol. 29, **2004**, p. 1
[10] Bischoff, J.L., Pitzer, K.S., Am. J. Sci., Vol. 289, **1989**, p. 217
[11] Armellini, F.J., Tester, J.W., Fluid Phase Equilib., Vol. 84, **1993**, p. 123
[12] DiPippo, M.M., Sako, K., Tester, J.W., Fluid Phase Equilib., Vol. 157, **1999**, p. 229
[13] Weber, M.*, et al.*, Corrosion/NACE 2001, 56th Annual Conference & Exposition, Houston, TX, USA, **2001**, (Paper No.01370)
[14] Lieball, K., Doctoral thesis, Swiss Federal Institute of Technology (ETH) Zurich, Switzerland, No. 14911, **2003 (http://www.e-collection.ethz.ch)**
[15] Wellig, B., Doctoral thesis, Swiss Federal Institute of Technology (ETH) Zurich, Switzerland, no. 15'038, **2003 (http://www.e-collection.ethz.ch)**
[16] Wellig, B., Lieball, K., von Rohr, P.R., J. Supercrit. Fluids, Vol. 34, **2005**, p. 35
[17] Schilling, W., Franck, E.U., Ber. Bunsen-Ges. Phys. Chem. Chem. Phys., Vol. 92, **1988**, p. 631
[18] Hirth, T., Franck, E.U., Ber. Bunsen-Ges. Phys. Chem. Chem. Phys., Vol. 97, **1993**, p. 1091
[19] Pohsner, G.M., Franck, E.U., Ber. Bunsen-Ges. Phys. Chem. Chem. Phys., Vol. 98, **1994**, p. 1082
[20] Franck, E.U., Wiegand, G., Pol. J. Chem., Vol. 70, **1996**, p. 527
[21] Steeper, R.R.*, et al.*, J. Supercrit. Fluids, Vol. 5, **1992**, p. 262
[22] Steeper, R.R.*, et al.*, Methane and methanol diffusion flames in supercritical water, Sandia National Laboratories, SAND92-8474, **1992**
[23] Serikawa, R.M.*, et al.*, Fuel, Vol. 81, **2002**, p. 1147
[24] La Roche, H.L., Weber, M., Trepp, C., Chem. Eng. Technol., Vol. 20, **1997**, p. 208
[25] Weber, M., Wellig, B., Rudolf von Rohr, P., Corrosion/NACE '99, 54th Annual Conference & Exposition, San Antonia, TX, USA, **1999**, (Paper No.258)